Trace-element fractionation by impact-induced volatilization: SIMS study of lunar HASP samples

J.J. Papike, M.N. Spilde, C.T. Adcock, G.W. Fowler, and C.K. Shearer

Institute of Meteoritics, Department of Earth and Planetary Sciences, University of New Mexico,
Albuquerque, New Mexico 87131-1126, U.S.A.

Abstract

Impact is a dominant process acting on the surfaces of planetary bodies and is the major process that modifies the physical and chemical nature of planetary materials on atmosphere-free bodies once volcanic activity has ceased. Elements with relatively high volatilities are readily mobilized during impact. HASP (high alumina, silica poor) compositions are thought to be generated by impact-induced volatilization processes on the moon. The high Al/Si ratio of HASP is believed to be the result of preferential loss of SiO_2 relative to Al_2O_3. Here we report SIMS analyses for HASP glass beads and devitrified glasses from the Apollo 14 regolith to assess the behavior of Li, Be, B, REE, Sr, Y, and Zr during impact events. We compare the behavior of these trace elements to the behavior of major and minor elements analyzed by the electron microprobe. The HASP samples we studied fall into two compositional groups with one group apparently derived from KREEPy lunar lithologies and the other from anorthosite. The KREEPy HASP beads have an estimated mass loss of 28% compared to their KREEPy protolith. We estimate that 44% of SiO_2 and 35% of FeO were lost during impact-induced volatilization. The mass loss estimate for the anorthositic protolith to produce anorthositic HASP is more uncertain because of the uncertainity of the protolith composition. However, an estimate of ~25% appears reasonable with 38% loss of silica. Clearly, impact processes, in the early stages of planetary evolution, are important in the modification of geochemical signatures, and ordinarily geochemically coherent elements may be decoupled because of different volatilities.

Introduction

Impact is the dominant process acting on the surfaces of atmosphere-free planetary bodies once volcanic activity has ceased. It is the process that modifies both the physical and chemical character of planetary surface materials. The phenomenon of volatile element transport by impact was identified early in the study of Apollo samples (e.g., Ivanov and Florensky 1975; Naney et al. 1976). Naney et al. (1976) systematically described and named an impact glass type with an unusually high-Al and Si-poor nature and referred to it as HASP. Since the Naney et al. (1976) description of HASP glass, this glass type has been found in many Apollo lunar soils and breccias and in lunar meteorites (Warren and Kallemeyn 1995). HASP glass beads appear to increase in abundance in the finer soil fractions. For example, Keller and McKay (1992) studied glass spheres from a mature highland soil (Apollo 16, Sample 61181) using a transmission electron microscope and found that the majority of the glasses analyzed in the <20 μm size fraction have refractory, HASP compositions. Keller and McKay (1992) also identified a group of volatile-rich, alumina-poor glasses which they named VRAP. They interpreted the VRAP glasses to be the complementary condensates to the volatile-depleted HASP glasses.

Vaniman (1990) did a thorough study of glass variants and HASP trends in Apollo 14 regolith breccias. The work of Vaniman forms the basis for our present study. We used the identical suite of thin sections, and Vaniman's photodocumentation guided us to the locations of the larger HASP fragments. Additional HASP fragments were searched for and found by an automated electron microprobe search (Adcock et al. 1997). In addition to HASP glasses, Vaniman (1990) and Vaniman and Bish (1990) reported the occurrence of devitrified HASP compositions in a specific regolith breccia (14076,5) and named a new lunar mineral, yoshiokaite, based on study of the devitrification products. The same yoshiokaite fragments analyzed by these authors were also analyzed in our study.

The chemical systematics identified in HASP compositions are likely the result of differential volatilization (Ivanov and Florensky 1975; Naney et al. 1976; Delano et al. 1981). Boschelli and McKay (1987) conducted an experimental study on lunar simulant glasses to explain better the volatilization process. They found that the process could be modeled by Rayleigh fractionation. Their experiments showed a significant loss of Si and Fe with complementary increases in Ca, Mg, and Al.

In our present study, we focus on the behavior of a

group of trace elements with different volatilities in HASP materials. An early report on this research was presented by Papike et al. (1997).

EXPERIMENTAL METHODS

To search for HASP glasses and to acquire the electron microprobe (EMP) analyses, we used a JEOL 733 Superprobe equipped with an Oxford eXL II analyzer and an Oxford/Link EDS system. The Oxford analyzer system includes a software package called Featurescan™ that defines discrete features within a field of view in the back-scattered electron (BSE) image. Chemical criteria are based on previous HASP studies (Vaniman 1990) where HASP beads are defined as having Al_2O_3 contents of greater than 16 wt% and SiO_2 contents of less than 40 wt%. All grains that passed the Featurescan classification were further filtered offline by their EDS quantitative analyses in a spreadsheet. This additional filtering step was necessary as some sections contained numerous glass fragments with a composition close to that of HASP. Finally, the locations in the data file of those features that had passed this last filtering step were revisited and analyzed by WDS for major and minor elements. All WDS analyses were performed at an accelerating voltage of 15 kV and a beam current of 20 nA using natural element standards and a ZAF correction routine. Analyses of fragments large enough (>20 μm) to fully contain the SIMS beam are reported in Table 1. A total of 30 HASP beads and fragments were found by this method during a search of 13 samples examined from the Apollo 14 suite (Adcock et al. 1997).

SIMS analyses of HASP glass were conducted using a Cameca IMS 4f ion microprobe. HASP glasses were analyzed for the trace elements Li, Be, B, Sr, Y, Zr, La, Ce, Nd, Sm, Eu, Dy, Er, and Yb. For clarity in plotting REE patterns with Eu anomalies, concentrations of Gd were estimated using simple interpolation between Sm and Dy.

Analyses were made by bombardment of the sample with primary O^- ions accelerated through a nominal potential of 17 kV. A primary ion current of 10–20 nA was focused on the sample over a spot diameter of 15–25 μm. A 150 μm secondary ion image field was used in conjunction with a 33 μm field aperture. Sputtered secondary ions were energy filtered using an energy window of 50 V and a sample offset voltage of −75 V. This degree of energy filtering suppresses all significant isobaric interferences for the elements analyzed in this study (Shimizu et al. 1978).

Each analysis involved repeated cycles of peak stepping through $^7Li^+$, $^9Be^+$, $^{11}B^+$, and $^{30}Si^+$, (first package) or $^{30}Si^+$, $^{88}Sr^+$, $^{89}Y^+$, $^{90}Zr^+$, $^{139}La^+$, $^{140}Ce^+$, $^{146}Nd^+$, $^{147}Sm^+$, $^{151}Eu^+$, $^{153}Eu^+$, $^{163}Dy^+$, $^{167}Er^+$, and $^{174}Yb^+$ (second package). Both packages included counting on a background position to monitor detection noise. Absolute concentrations of each element were then calculated using empirical relationships between measured peak/$^{30}Si^+$ ratios (normalized to known SiO_2 content) and elemental concentrations, as derived from daily calibration measure-
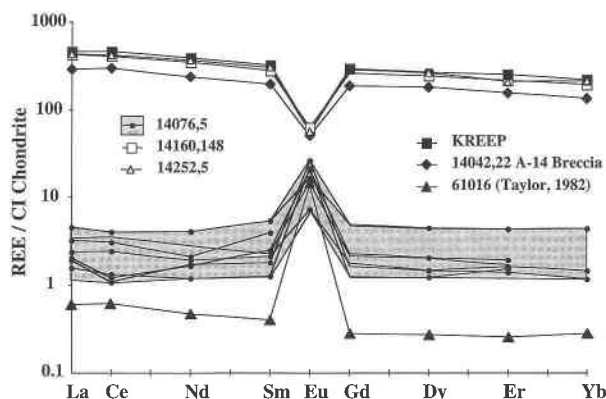

FIGURE 1. Chondrite normalized (Anders and Grevesse 1989) REE for KREEPy and anorthositic HASP glasses together with their assumed protolith REE concentrations.

ments of documented basaltic glass standards JDF-D2 for the first analytical package (Shearer et al. 1994) and AII-93-11-103 for the second analytical package (Newsom et al. 1986).

Peak counting times were varied to optimize precision. For the REE, the observed internal precisions are typically better than 5–10% at chondrite concentrations. In the case of the other trace and minor elements, precisions were typically better than 1–2%.

All ion microprobe analyses were conducted at locations previously analyzed by EMP, and the SiO_2 concentrations determined by EMP were used in reducing the SIMS data. Inclusion of contaminating phases in the SIMS analyses was avoided by selecting optically clean HASP fragments and by mass imaging of major elements before and after each spot SIMS analysis.

RESULTS AND DISCUSSION

Eleven HASP fragments were identified in our electron microprobe search that were large enough to be analyzed by SIMS. Their EMP and SIMS analyses are presented in Table 1. HASP fragments from samples 14160 and 14252 are lower in Al_2O_3 than those in 14076 and have the signature of KREEP (Warren 1989). The protolith for these glasses could have been Apollo 14 KREEPy soils, breccias, or both (Vaniman 1990). HASP fragments from sample 14076 are distinctly higher in Al_2O_3 and more likely derived from anorthositic protolith (Vaniman 1990; Vaniman and Bish 1990). Table 1 shows that Zr, Y, Be, and Li are in higher concentrations in the KREEPy HASP glasses than in the anorthositic HASP glasses. Table 2 presents possible KREEPy and anorthositic protolith compositions.

Figure 1 illustrates REE systematics. The KREEPy HASP glasses (samples 14160 and 14252) have elevated REE concentrations almost identical to the high-K KREEP of Warren (1989). The assumed KREEPy protolith (sample 14042, Table 2) is also shown for reference. The anorthositic HASP glasses have much lower REE concentrations than the KREEPy HASP glasses.

TABLE 1. Elemental concentrations of Apollo 14 HASP glasses

Thin section	Bead no.	SiO$_2$	TiO$_2$	Al$_2$O$_3$	FeO	MgO	CaO	Na$_2$O	K$_2$O
					Weight percent				
14076,5	V-07	35.3	0.13	42.7	0.63	0.65	21.0	0.01	0.02
14076,5	V-13	27.1	0.10	46.3	0.03	0.23	26.0	0.20	0.01
14076,5	V-14	33.4	0.26	39.5	0.27	2.30	24.8	0.05	0.00
14076,5	V-18	22.4	0.08	53.2	0.07	1.47	23.2	0.07	0.00
14076,5	V-21	19.5	0.09	52.2	0.00	0.18	28.8	0.02	0.00
14076,5	V-43	27.6	0.07	46.3	0.02	0.08	25.4	0.36	0.00
14160,148	V-03	37.7	2.05	23.8	8.43	11.6	15.2	0.00	0.00
14160,148	V-06	35.6	2.44	22.5	10.1	11.8	14.5	0.00	0.00
14252,5	I-03	40.1	2.23	22.1	9.97	12.0	13.5	0.00	0.00
14252,5	I-07	36.3	2.48	22.5	10.4	12.9	14.1	0.00	0.00
14252,5	V-07	38.5	2.49	22.7	10.3	11.5	14.0	0.01	0.00

However, their REE concentrations are elevated relative to the assumed protolith values (sample 61016, Fig. 1). Thus the REE for the HASP fragments are enriched in REE relative to their likely protoliths.

Figure 2a is a spider diagram that compares the average analysis (Table 1) of KREEPy HASP glass to its estimated protolith composition and Figure 2b compares the average analysis (Table 1) of anorthositic HASP glass to its assumed protolith composition. If there were no mass loss or gain in a process that alters a lithology from its original protolith composition, then compositions plotting above 0.5 would indicate enrichments relative to protolith compositions while values plotting below 0.5 would indicate depletions. However, when mass loss is involved, as in the process of volatilization, these diagrams can only be used in a qualitative way. For example, Figure

TABLE 2. Assumed protolith compositions for HASP

	Anorthosite*	KREEPy Regolith†
	Weight percent	
SiO$_2$	45.0	47.95
TiO$_2$	0.02	1.75
Al$_2$O$_3$	34.6	17.9
FeO	0.30	11.0
MnO	0.10	0.15
MgO	0.20	9.1
CaO	19.6	11.0
Na$_2$O	0.40	0.67
K$_2$O	0.01	0.48
Total	100.23	100.0
	Parts per million	
La	0.14	68.4
Ce	0.37	180
Nd	0.21	108
Sm	0.058	28.8
Eu	0.77	2.82
Gd	0.054	—
Dy	0.065	44
Er	0.040	—
Yb	0.045	22
Lu	0.01	2.80
Li	—	14
Be	—	6.6
B	—	10
Sr	180	184
Y	—	267
Zr	2.4	810

* Data reported in Taylor (1982). Anorthosite 61016.
† Data from Simon et al. (1989), Table 5, Sample 14042,22 and Hasken and Warren (1991).

2a indicates that SiO$_2$, FeO, Na$_2$O, K$_2$O, and B are depleted relative to the other plotted elements. These depletions are consistent with the process of differential volatilization by Raleigh fractionation (Boschelli and McKay 1987). For the anorthositic HASP beads the systematics are more complicated. Although it is clear that SiO$_2$, FeO, and Na$_2$O show the greatest depletions, Al$_2$O$_3$, CaO, Sr, and Eu also appear depleted relative to TiO$_2$, MgO, Zr, and the REE (excluding Eu).

More quantitative estimates of elemental gains and losses are made possible using an isocon diagram (Grant 1986). Figure 3a plots the concentration of elements in the KREEPy HASP glass vs. its assumed protolith compositions. Concentrations of elements and oxides are approximately scaled so all will plot on one diagram. If there were no elemental gains or losses, all points would plot along an isocon line at 45°. However, if there are elemental losses, as necessitated by a volatilization process, other systematics occur. The immobile or refractory elements will define an isocon whose slope gives an estimate of mass loss. In Figure 3a the slope of the isocon is 1.38 which equals M$^{\text{O}}$/M$^{\text{A}}$ (mass of original rock or protolith/mass of the altered rock). This is equivalent to M$^{\text{A}}$/M$^{\text{O}}$ = 0.72 or a mass loss of ~28%. Once an isocon is established, the relative gains or losses of any element are determined by their proportional displacements from the isocon. Thus we estimate that ~44% of SiO$_2$, and ~35% of FeO, were lost during the volatilization process that converted a KREEP-rich protolith to KREEPy HASP. These mass losses alone account for 26% mass loss from the KREEPy protolith. When we subtract the mass losses of SiO$_2$ and FeO from the protolith composition (Table 2) and renormalize the analyses to 100%, we predict an analyses very close to the KREEPy HASP analysis reported in Table 1. This closure in our calculations is an independent check on the isocon method because the isocon slope is determined from the behavior of the refractory elements only.

Assessment of the systematics for the anorthsitic HASP materials is more complicated because our choice for the protolith composition is more uncertain than for the KREEPy HASP. A small amount of KREEP in the anorthositic protolith will significantly change the trace-element systematics. The spider diagram (Fig. 2b) shows

TABLE 1.—*Extended*

Thin section	Bead no.	Li	Be	B	Sr	Y	Zr	La	Ce	Nd	Sm	Eu	Dy	Er	Yb
							Parts per million								
14076,5	V-07	1.24	0.26	0.08	362	1.51	3.17	0.76	1.83	0.95	0.57	1.11	—	—	—
14076,5	V-13	4.74	0.14	0.15	222	1.43	2.35	0.37	0.79	0.53	0.18	1.20	0.29	0.24	0.13
14076,5	V-14	4.76	0.20	1.77	183	5.63	15.6	1.06	2.41	1.83	0.79	0.94	1.07	0.69	0.71
14076,5	V-18	—	0.17	0.04	247	1.66	2.84	0.47	0.72	0.74	0.37	1.16	0.50	0.30	0.17
14076,5	V-21	0.04	0.14	0.04	290	2.04	3.29	0.45	0.65	0.77	0.27	1.47	0.35	0.22	0.19
14076,5	V-43	3.72	0.25	3.43	119	2.40	7.23	0.56	1.45	0.86	0.31	0.40	0.35	0.25	0.24
14160,148	V-03	14.6	8.2	0.59	264	307	1309	95	232	148	39.5	3.58	54.7	32.8	30.2
14160,148	V-06	14.0	9.04	1.00	292	351	1468	106	263	168	44.1	3.47	64.7	36.3	33.3
14252,5	I-03	13.2	8.22	2.21	254	337	1296	106	271	173	49.1	2.35	66.1	35.1	35.8
14252,5	I-07	13.4	7.78	0.81	276	343	1400	106	261	168	45.5	3.87	67.1	33.7	35.7
14252,5	V-07	16.0	7.55	0.57	282	312	1319	94.9	238	159	39.4	—	61.4	32.0	33.2

that species normally considered refractory such as Al_2O_3, CaO, Sr, and Eu appear depleted relative to TiO_2, MgO, Zr, and the other REE (excluding Eu). However, this appearence could be due to the wrong choice for the protolith composition with respect to these elements. More quantitative insights into the volatilization process that produced anorthositic HASP glass from anorthosite pro-

tolith are provided by the isocon diagram (Fig. 3b). An isocon fit through the REE (excluding Eu), MgO, Zr, and TiO_2 has a slope of 4.27 or $M^A/M^O = 0.23$ indicating a mass loss of 77%! However, a second isocon that includes CaO, Al_2O_3, and Sr appears more credible. This isocon has a slope of 1.34 indicating a mass loss of ~25%. The estimated loss of SiO_2 is 38%. The other higher isocon with slope 4.27 apparently is a false isocon resulting from an estimate of the anorthositic protolith that is too low in the KREEP components, especially the REE.
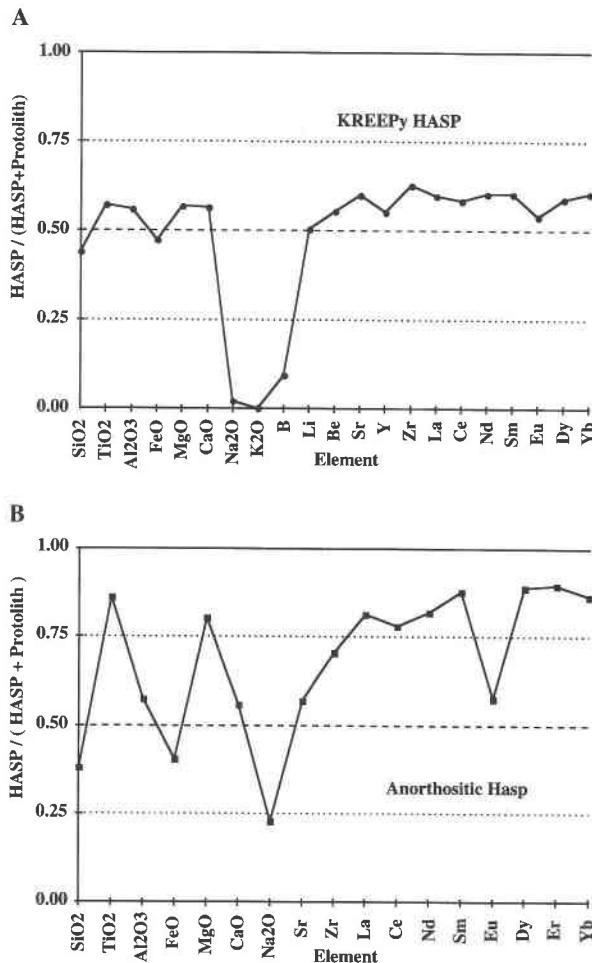

FIGURE 2. Spider diagrams for (A) KREEPy and (B) anorthositic HASP glasses. See text for discussion.
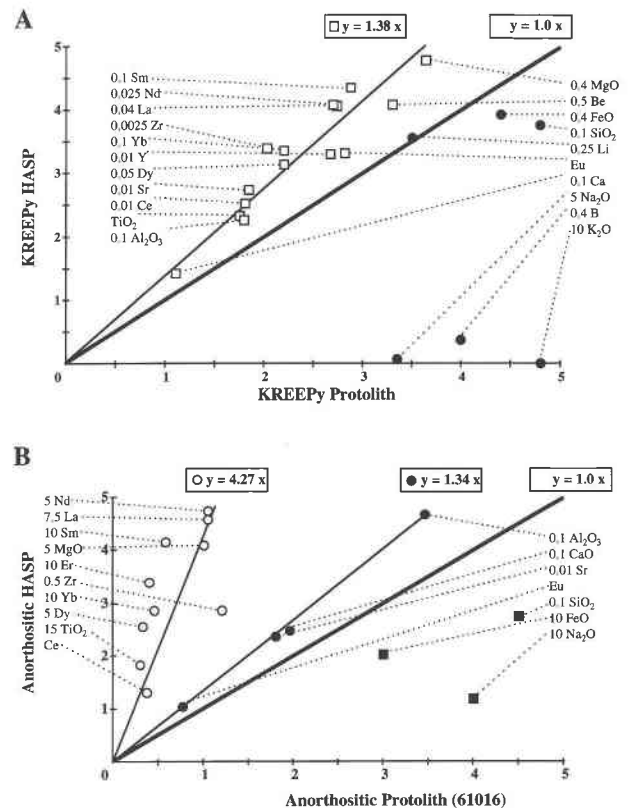

FIGURE 3. Isocon diagrams for (A) KREEPy and (B) anorthositic HASP glasses. See text for discussion. The number associated with each element is the scaling factor used to scale the data to fit the plot.

REFERENCES CITED

Adcock, C.T., Spilde, M.N., and Papike, J.J. (1997) Automated HASP glass search using the electron microprobe. Lunar and Planetary Science XXVIII, 5–6.

Anders, E. and Grevesse, N. (1989) Abundances of the elements: Meteoritic and solar. Geochimica et Cosmochimica Acta, 53, 197–214.

Boschelli, L.J. and McKay, D.S. (1987) Differential volatilization of lunar impact glass using Raleigh fractionation modeling. Lunar and Planetary Science XVIII, 109–110.

Delano, J.W., Lindsley, D.H., and Rudowski, R. (1981) Glasses of impact origin from Apollo 11, 12, 15 and 16: Evidence for fractional vaporization and mare/highland mixing. Proceedings of the Lunar and Planetary Science Conference, 12, 339–370.

Grant, J.A. (1986) The isocon diagram—A simple solution to Gresens' equation for metasomatic alteration. Economic Geology, 81, 1976–1982.

Haskin, L. and Warren, P. (1991) Lunar Chemistry. Lunar Sourcebook, Cambridge University Press, 357–474.

Ivanov, A.V. and Florensky, K.P. (1975) The role of vaporization process in lunar rock formation. Proceedings of the Lunar Science Conference, 6, 1341–1350.

Keller, L.P. and McKay, D.S. (1992) Micrometer-sized glass spheres in Apollo 16 soil 61181: Implications for impact volatilization and condensation. Proceedings of Lunar and Planetary Science, 22, 137–141.

Naney, M.T., Crowl, D.M., and Papike, J.J. (1976) The Apollo 16 drill core: Statistical analysis of glass chemistry and the characterization of a high alumina-silica poor (HASP) glass. Proceedings of the Lunar Science Conference, 7, 155–184.

Newsom, H.E., White, W.M., Jochum, K.P., and Hofmann, A.W. (1986) Siderophile and chalcophile element abundances in oceanic basalts, Pb isotope evolution and grown of the Earth's core. Earth and Planetary Science Letters, 80, 299–313.

Papike, J.J., Spilde, M.N., Adcock, C.T., Fowler, G.W., and Shearer, C.K. (1997) Trace element fractionation by impact-induced volatilization: SIMS study of lunar HASP glasses. Lunar and Planetary Science XXVIII, 1059–1060.

Shearer, C.K., Layne, G.D., and Papike, J.J. (1994) The systematics of light lithophile elements (Li, Be, and B) in lunar picritic glasses: Implications for basaltic magmatism on the Moon and the origin of the moon. Geochimica et Cosmochimica Acta, 58, 5349–5362.

Shimizu, N., Semet, M.P., and Allégre, C.J. (1978) Geochemical applications of quantitative ion-microprobe analysis. Geochimica et Cosmochimica Acta, 42, 1321–1334.

Simon, S.B., Papike, J.J. , Shearer, C.K., Hughes, S.S., and Schmitt, R.A. (1989) Petrology of Apollo 14 regolith breccias and ion microprobe studies of glass beads. Proceedings of the Lunar and Planetary Science Conference, 19, 1–17.

Taylor, S.R. (1982) Planetary Science: A lunar perspective. Lunar and Planetary Institute. 481 P.

Vaniman, D.T. (1990) Glass variants and multiple HASP trends in Apollo 14 regolith breccias Proceedings of the Lunar and Planetary Science Conference, 20, 209–217.

Vaniman, D.T. and Bish, D.L. (1990) Yoshiokaite, a new Ca, Al-silicate mineral from the moon. American Mineralogist, 75, 676–686.

Warren, P.H. (1989) KREEP: Major-element diversity, trace element uniformity (almost). Workshop on Moon in transition, Lunar and Planetary Institute Technical Report, 89-03, 149–153.

Warren, P.H. and Kallemeyn, G.W. (1995) QUE 93069: A lunar meteorite rich in HASP glasses. Lunar and Planetary Science XXVI, 1465–1466.